Ashdin Publishing
Journal of Transition Metal Complexes
Vol. 1 (2018), Article ID 236061, 7 pages
doi:10.4303/jtmc/236061

Research Article

Spectroscopic, Physical, Thermal, and Magnetic Studies of N-[Tris(Hydroxyl Methyl)Methyl]Glycine (Tricine, L) Complexes and Their Applications Against Tumor Activity

Eman A. Hassan, Nagwa Nawar, Ebrahim Abdel-Galil, and Mohsen M. Mostafa

Chemistry Department, Faculty of Science, Mansoura University, Egypt
Address correspondence to Mohsen M. Mostafa, amohsenmostafa@yahoo.com

Received 21 March 2018; Revised 9 April 2018; Accepted 10 April 2018

Abstract New metal complexes derived from the interaction of tricine with some metal salts (Cu^{2+}, Co^{2+}, Zn^{2+}, Cd^{2+}, and Ni^{2+}) were synthesized and characterized by spectral (IR, UV-vis., EPR, mass, ^{1}H-NMR), magnetic, conductance, and thermal (TGA measurements) analyses. The results suggest that **L** coordinates in a mono-, bi- and/or tridentate manners via the COO, NH, and OH groups. Also, the results suggest that the carboxylate group is bonded to the metal ions in two forms depending on the type of solvent and the pH of the reaction mixture. Spectral and magnetic studies suggest an octahedral geometry around the investigated metal ions. Moreover, **L** coordinates in a tridentate manner. Material studio program has been used for calculating HUMO, LUMO, and DFT parameters on the atoms to confirm the geometry of complexes. The cytotoxic activities of complexes against human tumor cells have been screened. The Cu^{2+} complex showed the highest activities using colorimetric assay.

Keywords tricine complexes; biological studies; anticancer studies; DFT calculations

1. Introduction

The structure of *N*-[tris(hydroxyl methyl)methyl]glycine (**L**) shows several coordination sites (COO, OH, and NH) and thence it acts as an excellent chelating agent [1]. Literature survey reveals that **L** has the ability to bind metal ions in mono-, bi- and/or tridentate manners [2, 3, 4, 5, 6, 7, 8, 9, 10, 11, 12]. In continuation of our earlier work [13] and others [14, 15], we extend this work to throw the light on the importance of tricine in different fields in particular biological studies. We previously reported that the participation of the coordination sites depends on the pH [13] during complex formation but we reported herein that the coordination sites depend also on the type of the solvent used. Moreover, the aim of this work is to synthesize and characterize new series of its complexes involving Zn^{2+}, Cu^{2+}, Cd^{2+}, Ni^{2+}, and Co^{2+} salts, which are not reported earlier in literature, involving structural explication, thermal, physical behavior, spectral and molecular modeling of complexes. Finally, one of our goals is to study the cytotoxic activity of the metal complexes.

2. Experimental

2.1. Instrumentation and materials

All the chemicals and solvents and instrumentation were carried out as reported earlier [13].

2.2. Synthesis of solid complexes

Two categories of solid complexes were synthesized and characterized. The first type of solid complexes was prepared in absolute EtOH while the second type was isolated from redistilled H_2O. The complexes separated in presence of H_2O are accompanied by losing a proton from the carboxylic group as in case of Co^{2+} and Ni^{2+} complexes at pH = 8 using NaOH and NaOAc as buffering agents, respectively. On the other hand, the Co^{2+} and Ni^{2+} complexes separated in presence of absolute EtOH as a solvent and the ligand participates without losing a proton from the carboxylic group at pH above 8.

2.2.1. Synthesis of complexes in EtOH

A hot EtOH solution of the metal chlorides $CuCl_2 \cdot 2\,H_2O$ (1.0 mmol, 0.851 g), $NiCl_2 \cdot 6\,H_2O$ (0.59 g), and $CoCl_2 \cdot 6\,H_2O$ (0.59 g) was added to hot solution of **L** (1.0 mmol, 0.896 g) dissolved in EtOH (25 mL) and few drops of redistilled H_2O. The pH of the reaction mixture was adjusted with sodium acetate in case of Cu^{2+}, while in case of Co^{2+} and Ni^{2+} complexes NaOH was used to raise the pH of the reaction mixture up to 8. The reaction mixture was refluxed on hot plate for 3 h. The complexes formed were filtered off, washed several times with EtOH and diethyl ether, and finally dried in vacuum desiccator over anhydrous $CaCl_2$. The Cu^{2+} complex is readily soluble in redistilled H_2O and DMSO and partially soluble in EtOH and DMF, but Ni^{2+} and Co^{2+} complexes are partially soluble in H_2O, EtOH, DMSO, and DMF.

2.2.2. [Co(tric)$_2$Cl$_2$] · 2.5H$_2$O

Yield: 90%; brown powder; MP > 300 °C. IR (KBr; cm^{-1}): 3,415, 3,227 [OH (H$_2$O)], OH (EtOH), 2,966 (NH), 2,880 (OH, acid), 1,602 (CO), 521 (M−O). Calcd.: for $C_{12}H_{30}CoN_2O_{12}Cl_2$ (%): C, 27.5; H, 5.76; Co, 11.24, Cl, 13.52. Found: C, 26.8; H, 5.46; Co, 11.49, Cl, 13.00. Λ_m (DMSO): 8 Ω^{-1}cm^{2}mol^{-1}. μ_{eff}: 5.1 BM. UV (cm^{-1}): 25,252 (LMCT), 18,726 [$^4A_{2g}$(F) → $^4T_{1g}$(P); ν_3], 16,666 ($^4A_{2g}$ → $^4T_{1g}$; ν_2). The values of ν_1 ($^4A_{2g}$ → $^4T_{2g}$; ν_1), B, and β were calculated and found to be 8,928 cm^{-1}, 400 cm^{-1}, and 0.41, respectively. The β value indicates that the bond between the **L** and Co^{2+} ion is covalent in nature.

2.2.3. [Cu(tric)$_2$Cl$_2$] · 3 H$_2$O

Yield: 95%; torques powder; MP 195 °C. IR (KBr; cm^{-1}): 3,322, 3,235 [OH (H$_2$O)], OH (EtOH), 2,895 (OH, acid), 2,968 (NH), 1,620 (CO), 557 (M−O). Calcd.: for $C_{12}H_{32}CuN_2O_{13}Cl_2$ (%): C, 26.35; H, 5.9; Cu, 11.62, Cl, 12.96. Found: C, 26.14; H, 5.42; Cu, 11.5, Cl, 13.3. Λ_m (DMSO): 65 Ω^{-1}cm^{2}mol^{-1}. μ_{eff}: 2.3 BM. UV (cm^{-1}): 31,847 (LMCT), 12,626 (^2E_g → $^2T_{2g}$). $g_{//} = 2.2$, $g_\perp = 2.11$, $G = 2.578$, and $A = 97.5$.

2.2.4. [Ni(tric)$_2$Cl$_2$(H$_2$O)$_2$] · H$_2$O

Yield: 50%; grass green powder; MP > 300 °C. IR (KBr; cm^{-1}): 3,311, 3,423 [OH (EtOH)], OH (H$_2$O), 3,254 (NH), 2,870 (OH, acid), 1,612 (CO), 512 (M−O). Calcd.: for $C_{12}H_{32}NiN_2O_{13}Cl_2$ (%): C, 26.59; H, 5.95; Ni, 10.82, Cl, 13.08. Found: C, 26.45; H, 5.03; Ni, 11.4, Cl, 13.82. Λ_m (DMSO): 3 Ω^{-1}cm^{2}mol^{-1}. μ_{eff}: 4.13 BM. UV (cm^{-1}): 29,940 (LMCT), 26,315 [$^3A_{2g}$ → $^3T_{1g}$(P); ν_3], 15,772 ($^3A_{2g}$ → $^3T_{1g}$; ν_2. The values of ν_1 ($^3A_{2g}$ → $^3T_{2g}$), B, and β were calculated and found to be 9,968 cm^{-1}, 812 cm^{-1}, and 0.78, respectively. The value of β suggests that the bond between the ligand and Ni^{2+} ion is mainly ionic in nature.

2.3. Synthesis of Co^{2+}, Ni^{2+}, Cd^{2+}, and Zn^{2+} complexes in redistilled H$_2$O

The complexes synthesized in the presence of H$_2$O are completely different from the above solid complexes isolated from EtOH. A hot aqueous solution of $ZnCl_2$ (1.0 mmol, 0.68 g) was added to hot solution of tricine (1.0 mmol, 0.90 g) dissolved in H$_2$O (25 mL) and few drops of ethanol. The reaction mixture was refluxed on hot plate for 6 h. The white product was filtered off and preserved in a desiccator over anhydrous calcium chloride. Cadmium acetate (1.0 mmol, 1.33 g), $NiCl_2 \cdot 6H_2O$ (0.59 g), and $CoCl_2 \cdot 6H_2O$ (0.59 g) were used to prepare the complexes using the same method of Zn^{2+} complex, but in the case of Co^{2+} and Ni^{2+} the pH was raised to 8 using NaOAc; μ_{eff} diamagnetic in the cases of Cd^{2+} and Zn^{2+} complexes.

2.3.1. [Cd(tric)$_2$(Ac)$_2$] · H$_2$O

Yield: 95%; white powder; MP > 238 °C. IR (KBr; cm^{-1}): 3,430 (OH, H$_2$O), 3,328 (OH, EtOH), 3,213 (NH), 2,922 (OH, acid), 1,604 (CO), 528 (M−O). Calcd.: for $C_{16}H_{34}CdN_2O_{15}$ (%): C, 31.66; H, 5.65; Cd, 18.52. Found: C, 31.07; H, 5.39; Cd, 18.08. Λ_m (DMSO): 0 Ω^{-1}cm^{2}mol^{-1}, U_{eff}: diamagnetic.

2.3.2. [Co(tric-H)$_2$] · 0.5H$_2$O

Yield: 80%; simon powder; MP > 300 °C. IR (KBr; cm^{-1}): 3,323 (OH, H$_2$O), 3,226 (OH, EtOH), 2,969 (NH), 2,828 (OH, acid), 1,614 (CO), 521 (M−O). Calcd.: for $C_{12}H_{25}CoN_2O_{21/2}$ (%): C, 33.97; H, 5.93; Co, 13.89. Found: C, 33.97; H, 6.16; Co, 13.65. Λ_m (DMSO): 2 Ω^{-1}cm^{2}mol^{-1}. μ_{eff}: 4.6 BM. UV (cm^{-1}): 23,041 (LMCT), 18,656 [$^4A_{2g}$(F) → $^4T_{1g}$(P); ν_3], 16,756 ($^4A_{2g}$ → $^4T_{1g}$; ν_2). The values of ν_1 ($^4A_{2g}$ → $^4T_{2g}$), B, and β were calculated and found to be 8,917 cm^{-1}, 413 cm^{-1}, and 0.42, respectively. The value of β suggests that the bond between the ligand and Co^{2+} ion is covalent in nature.

2.3.3. [Ni(tric-H)$_2$(H$_2$O)$_2$]

Yield: 50%; pale blue powder; MP > 300 °C. IR (KBr; cm^{-1}): 3,332 (OH, H$_2$O), 3,213 (OH, EtOH) 2,976 (NH), 2,890 (OH, acid), 1,601 (CO), 523 (M−O). Calcd.: for $C_{12}H_{28}NiN_2O_{12}$ (%): C, 31.95; H, 6.25; Ni, 13.01. Found: C, 32.38; H, 6.23; Ni, 13.8. Λ_m (DMSO): 0 Ω^{-1}cm^{2}mol^{-1}. μ_{eff}: 3.79 BM. UV (cm^{-1}): 24,752 [$^3A_{2g}$ → $^3T_{1g}$(P); ν_3], 15,479 ($^3A_{2g}$ → $^3T_{1g}$; ν_2). The values of ν_1 ($^3A_{2g}$ → $^3T_{2g}$), B, and β were calculated and found to be 10,466 cm^{-1}, 589 cm^{-1}, and 0.66, respectively. The value of β suggests that the bond between the ligand and Ni^{2+} ion is intermediate in nature.

2.3.4. [Zn(tric)$_2$Cl$_2$] · EtOH

Yield: 95%; white powder; MP > 300 °C. IR (KBr; cm^{-1}): 3,346 (OH, EtOH), 3,105 (NH), 2,868 (OH, acid), 1,614 (CO), 504 (M−O). Calcd.: for $C_{14}H_{32}ZnN_2O_{11}Cl_2$ (%): C, 31.1; H, 5.96; Zn, 12.09, Cl, 13.11. Found: C, 31.21; H, 5.63; Zn, 12.03. Λ_m (DMSO): 0 Ω^{-1}cm^{2}mol^{-1}. μ_{eff}: diamagnetic.

3. Results and discussion

3.1. IR spectra, electronic spectra, magnetic moments, and conductance studies

All the complexes derived from **L** and reported earlier in literature [1,2,3,4,5,6,7,8,9,10,11,12,13,14] show that the ligand coordinates to the metal ions in a mononuclear, binuclear, and tridentate manner. In our case, the results of spectral and magnetic measurements suggest also that **L** coordinates in a mono, bi- and/or tridentate manner and the isolated complexes have an octahedral structure

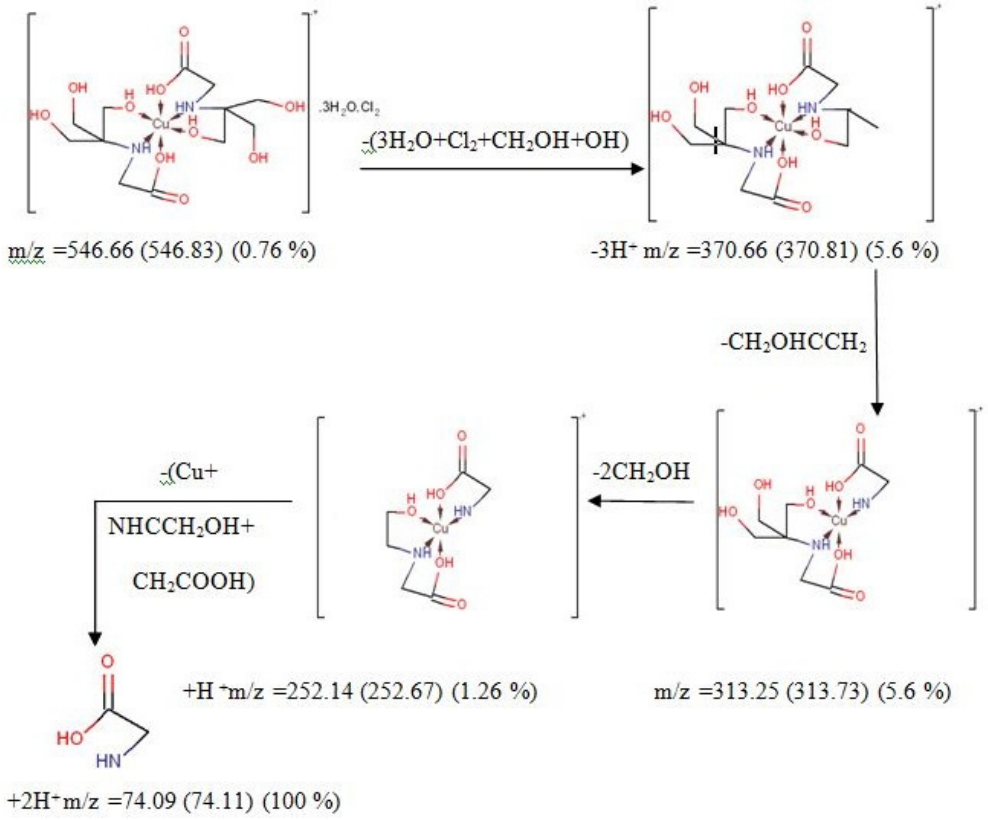

Scheme 1: The fragmentation pattern of $[Cu(tric)_2]Cl_2 \cdot 3\,H_2O$.

around the metal ions. The most assignment bands in the IR of tricine (Figure S1) was compared with the IR spectrum of the Ni^{2+} complex, $[Ni(tric)_2Cl_2(H_2O)_2] \cdot H_2O$ (Figure S2). The results indicate that **L** coordinates to the Ni^{2+} ion in a monodentate manner coordinating through the carboxylate oxygen group without displacement of a hydrogen atom from that group. Also, the IR spectra of the other complexes: $[Co(tric)_2Cl_2] \cdot 2.5H_2O$ (Figure S3), $[Zn(tric)_2Cl_2] \cdot EtOH$ (Figure S4), $[Cd(tric)_2(Ac)_2] \cdot H_2O$ (Figure S5), and $[Ni(tric\text{-}H)_2(H_2O)_2]$ (Figure S6), indicate that **L** coordinates in a bidentate manner while $[Cu(tric)_2]Cl_2 \cdot 3\,H_2O$ (Figure S7), $[Co(tric\text{-}H)_2] \cdot 0.5H_2O$ (Figure S8), and $[Ni(tric)_2Cl_2(H_2O)_2] \cdot H_2O$ (Figure S9) indicate that **L** coordinates in a tridentate manner [15, 16, 17]. The loss of a proton from the tricine on coordination depends on the solvent used (H_2O, EtOH) and the pH. The loss of proton in case of $[Co(tric\text{-}H)_2] \cdot 0.5H_2O$ and $[Ni(tric\text{-}H)_2] \cdot 2\,H_2O$ occurred on using H_2O as a solvent while with the rest of complexes the ligand reacted without losing a proton. This phenomenon is explained on the basis that the water molecules form weak hydrogen bonding with the active centers and hence it acts as a strong acid while the presence of ethanol makes tricine acts as a weak acid. This behavior causes a strong stabilization of the Zwiterrion. This behavior agrees with the results reported by Bates et al. [18].

The electronic spectra of all complexes were carried out in Nujol mull as shown in Figures S10, S11, S12, and S13. The results of electronic spectra as well as the values of magnetic moments indicate that the complexes have octahedral geometry around the metal ions [19, 20, 21]. The values of conductance (0–8 $ohm^{-1}\,cm^2\,mol^{-1}$) confirm that all the complexes are nonelectrolyte in nature [22] except the Cu^{2+} complex with the general formula, $[Cu(tric)_2]Cl_2 \cdot 3\,H_2O$, which is electrolyte in nature (1:2).

3.2. Mass spectra

The mass spectrum of $[Cu(tric)_2]Cl_2 \cdot 3\,H_2O$ at 120 °C (Figure S14) shows a molecular ion peak [m/z] at 546.66 and matches with the theoretical value (546.83). This proposes that the suggested structure of this complex is correct. The fragmentation pattern of the Cu^{2+} complex is shown in Scheme 1. Also, the results of elemental analyses and thermal analyses are taken as additional evidences for the proposed structure. The spectrum shows that the dissociation of Cu complex started with losing Cl_2, $3\,H_2O$, OH, and CH_2OH and giving protonated product at [m/z] 370.66. The protonated ligand ion appears to dissociate efficiently to give $OOC{-}CH_2{-}NH{-}Cu(OH)CO{-}CH_2{-}NH{-}C(CH_2OH)_3$ at [m/z] 252.14, which dissociate to give the signature product ion at [m/z] 74.09.

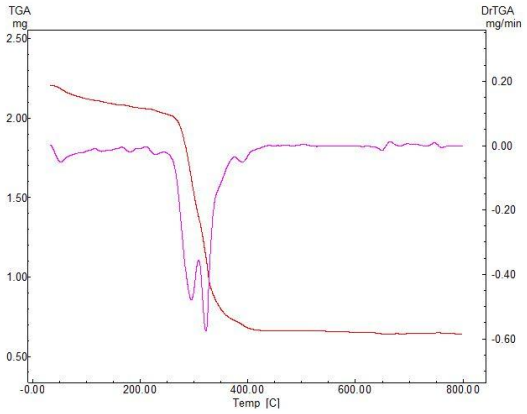

Figure 1: TGA, DTG curves of $[Co(tric)_2Cl_2] \cdot 2.5H_2O$.

3.3. Thermal studies

The thermal analyses (TGA and DTG) curves were performed under a temperature range from 20 °C up to 1,000 °C. The mass losses were estimated and computed up on the results of the TGA of the calculated mass loss using the results of the microanalyses. The four steps of the decomposition of $[Co(tric)_2Cl_2] \cdot 2.5H_2O$ complex is shown in Figure 1. The temperature of the first step from 25 °C to 135 °C corresponds to the loss of two H_2O molecules and CH_2 (Found: 8.632%, Calcd.: 9.55%). The temperature of the second and third steps from 135 °C to 800 °C is referred to the loss of the fragments ($C_9H_{22}N_2O_6 + 2\,HCl$) (Found: 62.199%, Calcd.: 62.036%). Finally, the residue appraises in the temperature range 800 °C–1,000 °C corresponds to $CoNO_4C$, in which the calculated loss 28.412% which is matching the found loss 29.1%. The thermal analyses curves of the other complexes are shown in Figures S15, S16, S17, and S18. All the thermal decomposition steps are tabulated in Table S1.

3.4. UV-vis. spectra

The electronic spectra of the Ni^{2+} and Co^{2+} complexes with the general formulae, $[Ni(tric)_2Cl_2(H_2O)_2] \cdot H_2O$, $[Co(tric\text{-}H)_2] \cdot 0.5H_2O$, and $[Ni(tric\text{-}H)_2(H_2O)_2]$, as an examples of the two types of the isolated solid complexes, show bands as shown in the experimental section. These bands suggest an octahedral geometry around the two metal ions (Ni^{2+} and Co^{2+}). Racah parameters (B and β) were calculated as reported earlier [13, 19].

3.5. EPR spectra

EPR spectrum of $[Cu(tric)_2]Cl_2 \cdot 3\,H_2O$ is given in Figure 2. The results of this complex are $g_{//} = 2.21$, $g_{\perp} = 2.1$, $G = 2.578$, and $A = 97.5$. The observed $g_{//}$ for the Cu complex is less than 2.3, suggesting important covalent character of the metal-ligand bond [23]. The direct $g_{//} > g_{\perp} > ge$ (2.0023) viewed for this complex suggests that d_{x2-y2} is the ground state of the Co^{2+} ion [24].

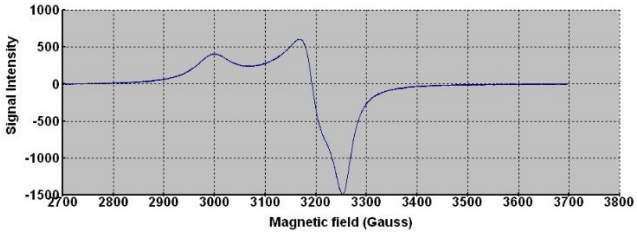

Figure 2: EPR spectrum of $[Cu(tric)_2]Cl_2 \cdot 3\,H_2O$.

3.6. Modeling

The molecular modeling drawing demonstrates the bond lengths, bond angles (Tables S2–S16), chemical reactivity, energy components (Kcal/mol), kinetic energy (Kcal/mol), and binding energy (Kcal/mol) of tricine and its metal complexes are shown in Tables 1 and 2 [24,25,26,27,28,29]. The DFT theory explains the results [24,25,26,27,28,29]. The molecular structures of tricine and its metal complexes are shown in Schemes S1–S8. The data of bond angles and lengths in Tables S2–16 illustrate the following comments.

(1) $[Co(tric\text{-}H)_2] \cdot 0.5H_2O$ (Scheme S1) has an octahedral structure in which **L** acts in a tridentate manner. The first coordinating case proceeds via O(7), N(12), and O(17). The second tricine coordinating case proceeds via O(5), N(8), and O(20), completing the octahedral structure around Co^{2+} ion. All the active groups turning in coordination have bonds longer than that existing in the ligand. There is a variety in N(12)−C(25), O(20)−C(10), N(8)−C(9), O(17)−C(4), and O(5)−C(13) bond lengths. They turn out to be changed because the coordination happens. N(12)−C(25), O(20)−C(10), and N(8)−C(9) bond distances in all complexes turn out to be longer due to the formation of M−N and M−O bonds. The bond angles of Co complex are close to octahedral geometry. The bond angles of tricine are modified up on coordination; the biggest change affects N(12)−C(25)−C(14), O(20)−C(10)−C(3), N(8)−C(9)−C(13), and O(5)−C(13)−C(9), which are decreased or expanded on complex formation as a result of bonding.

(2) As for the $[Co(tric)_2Cl_2] \cdot 2.5H_2O$ complex (Scheme S2), the cobalt atom has an octahedral geometry. The ligand of two tricine molecules acts in a bidentate manner coordinating via N(18), O(26), O(2), and N(11) and additionally two chloride ions Cl(5) and Cl(22) complete the octahedral structure. There is a huge change in N(18)−C(26), N(11)−C(13), O(26)−C(20), and O(2)−C(25). The bond angles of tricine are adjusted upon coordination and lessened or expanded on complex arrangement as a result of bonding such as C(12)−N(18)−C(16), C(10)−C(13)−N(11), C(26)−C(20)−O(3), and C(6)−C(13)−N(11).

Table 1: Calculated E_{HOMO}, E_{LUMO}, energy band gap (E_H-E_L), chemical potential (μ), electronegativity (χ), global hardness (η), global softness (S), and global electrophilicity index (ω) for tricine and its complexes.

Compound	E_HeV	E_LeV	(E_HE_L)eV	χeV	μeV	ηeV	SeV^{-1}	ωeV	σeV
L^1; $C_6H_{13}NO_5$	−5.180	−0.678	−4.502	2.929	−2.929	2.251	1.1255	1.9056	0.444
$[Co(L^1\text{-}H)_2]\cdot 0.5H_2O$	−5.503	−5.195	−0.308	5.349	−5.349	0.145	0.077	98.6613	6.8965
$[Co(L^1)_2Cl_2]\cdot 2.5H_2O$	−5.723	−5.150	−0.573	5.437	−5.4365	0.287	0.1433	51.580	3.490
$[Cu(L^1)_2]Cl_2\cdot 3\,H_2O$	−5.278	−4.958	−0.32	5.118	−5.118	0.16	0.08	81.856	6.25
$[Ni(L^1)_2(Cl)_2(H_2O)_2]\cdot H_2O$	−5.433	−5.328	−0.105	5.380	−5.380	0.0525	0.0262	275.66	19.047
$[Ni(L^1\text{-}H)_2(H_2O)_2]$	−5.561	−4.809	−0.752	5.185	−5.185	0.376	0.188	35.750	2.6595
$[Cd(L^1)_2(Ac)_2]\cdot H_2O$	−5.367	−1.942	−3.425	3.6545	−3.6545	1.7125	0.85625	3.89937	0.58394
$[Zn(L^1)_2Cl_2]\cdot EtOH$	−5.927	2.530	3.397	4.2285	−4.2285	1.6985	0.84925	5.2635	0.58875

(3) The $[Cu(tric)_2]Cl_2\cdot 3\,H_2O$ (Scheme S3) has an octahedral structure. The two ligands of tricine act in a tridentate manner chelating via O(6), O(8), N(14), N(19), O(4), and O(10). The bonds of all active groups joining in coordination are longer than that of currently existing ligand such as NH. There is a huge variety in N(19)−C(4), N(14)−C(21), O(8)−C(17), O(6)−C(11), O(3)−C(16), and O(10)−C(13) bond lengths. The bond angles are diminished or expanded on complex arrangement as an outcome of bonding such as C(21)−N(14)−C(13) and C(4)−C(11)−O(6).

(4) With the $[Ni(tric\text{-}H)_2(H_2O)_2]$ (Scheme S7), tricine is a bidentate ligand coordinating via O(23), O(7), N(16), and N(21). There is an extensive variety in N(16)−C(6), O(15)−C(17), and N(21)−C(1) bond lengths. The bond angles of tricine are very close to octahedral geometry. The bond angles are modified due to coordination. The bond angles are decreased or expanded on complex formation as a consequence of bonding, where the biggest change influences C(6)−C(13)−O(23), C(13)−C(6)−N(16), and C(1)−N(21)−C(17).

(5) $[Ni(tric)_2Cl_2(H_2O)_3]\cdot H_2O$ (Scheme S4) has an octahedral structure. Tricine acts in a monodentate manner coordinating via O(6) and O(26). The two chloride ions Cl(12), Cl(4) and two water molecules O(17) and O(19) complete the octahedral geometry. There is an extensive variety in O(6)−C(24) and O(26)−C(21) bond lengths. The bond angles C(2)−C(21)−O(26) and C(29)−C(24)−O(6) are decreased or expanded on complex formation as a consequence of bonding.

(6) The $[Zn(tric)_2Cl_2]\cdot EtOH$ (Scheme S5) has an octahedral structure. Tricine acts in a bidentate manner coordinating via N(5), N(10), O(8), and O(3). The two chloride ions Cl(1) and Cl(25) complete the octahedral structure around Zn^{2+} ion. There is a huge variety in N(5)−C(9), N(10)−C(9), O(8)−C(9), and O(3)−C(6) bond lengths. The bond angles are diminished or expanded on complex arrangement as an outcome of bonding such as C(4)−N(10)−C(24), C(24)−C(6)−O(3), C(14)−C(9)−O(8), and C(9)−C(14)−N(5).

(7) The $[Cd(tric)_2(Ac)_2]\cdot H_2O$ has an octahedral structure (Scheme S6). Tricine serves in a bidentate fashion coordinating via N(31), N(29), O(17), and O(33). The two acetate ions coordinating via its oxygenated ion O(2) and O(22) complete the octahedral structure around Cd^{2+} ion. The bond lengths N(31)−C(9), N(29)−C(9), O(17)−C(9), and O(33)−C(6) of complex are extensively varied in comparison with that of **L**. The bond angles C(4)−O(33)−O(13), O(10)−C(5)−O(17), C(23)−N(31)−C(18), and N(29)−C(8)−C(4) are lessened or expanded on complex as a result of bonding.

(8) Tricine (Scheme S7) and its bond angles and bond lengths are modified to some degree upon coordination. The bond distances in all isolated metal complexes turn to be longer due to the formation of M−O bond. The biggest change of bond angles affects O(2)−C(8)−O(12) and C(2)−N(9)−C(7).

Chemical reactivity

The assignment of energies of HOMO (π-donor) and LUMO (π-acceptor) are important parameters in quantum compound counts. The HOMO is the orbital that generally goes about as electron giver and the LUMO is the orbital that fundamentally goes about as electron acceptor. These molecular orbitals are also called frontier molecular orbitals (FMOs). The all negative values of E_{HOMO}, E_{LUMO}, and their neighboring orbitals show that the prepared molecules are steady. The energy gap (E_{HOMO}-E_{LUMO}) is an important stability index which serves to portray the chemical reactivity and kinetic stability of the molecule [30]. The gap (E_{HOMO}-E_{LUMO}) is connected to build up a hypothetical pattern for illustrating the structure in many molecular systems. The small gap in molecule means that the molecule is more polarized and the molecule is known as soft molecule. The responsive of soft molecules is more than that of the hard ones as they easily offer electrons to an acceptor. The small energy gap in tricine shows that charge transfer easily happens in it. The ability of the molecule to give electron is weaker if the HOMO energy value is low. On the opposite, the ability of the molecule is good if the HOMO energy value is high [31]. All the data are shown in Tables 1 and 2.

Table 2: Some of energetic properties of tricine and its complexes calculated by DMOL^3 using DFT method.

No.	Compound	HOMO (eV)	LUMO (eV)	Binding energy (kcal/mol)	Total energy (kcal/mol)	Kinetic energy (kcal/mol)
1	L^1; $C_6H_{13}NO_5$	−5.180	−0.678	−2483.726	-4.189×10^5	−3366.87
2	$[Co(L^1\text{-}H)_2]\cdot0.5H_2O$	−5.503	−5.195	−4627.657	-9.404×10^5	−6798.1629
3	$[Co(L^1)_2Cl_2]\cdot2.5H_2O$	−5.723	−5.150	−4850.727	-1.518×10^6	−6809.495
4	$[Cu(L^1)_2]Cl_2\cdot3\,H_2O$	−5.278	−4.958	−4485.746	-9.751×10^5	−8412.7703
5	$[Ni(L^1)_2Cl_2(H_2O)_2]\cdot H_2O$	−5.433	−5.328	−4846.830	-1.5353×10^6	−6758.1278
6	$[Ni(L^1\text{-}H)_2(H_2O)_2]$	−5.561	−4.809	−4617.265	-9.578×10^5	−6922.5730
7	$[Cd(L^1)_2(Ac)_2]\cdot H_2O$	−5.367	−1.942	−6209.948	-1.179×10^6	−7897.8359

Table 3: IC_{50} values of the isolated complexes.

Compounds	No.	In vitro cytotoxicity IC_{50} (μg/mL)	
		Hela	MCF-7
$[Co(tric\text{-}H)_2]\cdot0.5H_2O$	(1)	11.94	7.34
$[Co(tric)_2Cl_2]\cdot2.5H_2O$	(2)	41.39	44.23
$[Cu(tric)_2]Cl_2\cdot3\,H_2O$	(3)	48.2	58.0
$[Ni(tric)_2Cl_2(H_2O)_2]\cdot H_2O$	(4)	30.0	28.0
$[Ni(tric\text{-}H)_2(H_2O)_2]$	(5)	54.3	59.1
$[Cd(tric)_2(Ac)_2]\cdot H_2O$	(6)	23.48	14.3
$[Zn(tric)_2Cl_2]\cdot EtOH$	(7)	33.5	37.7
5-Fluorouracil		4.8	5.4

IC_{50} (μg/mL): 1–10 (very strong), 11–20 (strong), 21–50 (moderate), 51–100 (weak), and above 100 (noncytotoxic).

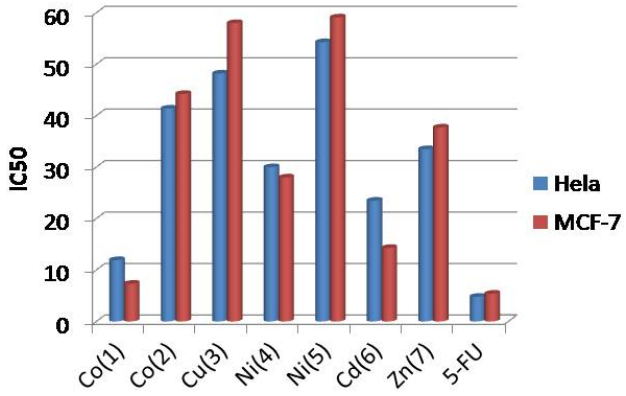

Figure 3: Scavenging capacities (IC_{50}) of metal complexes towards epithelioid carcinoma cervix cancer (Hela) and mammary gland breast cancer (MCF-7), 5-fluorouracil-standard antitumor.

3.7. Cell proliferation assay

According to the biological activity of Schiff bases, the capability of poly pyridyl complexes to inhibit cancer cell growth against epithelioid carcinoma cervix cancer (Hela) and mammary gland breast cancer (MCF-7) is appraised [32,33]. In our work, IC_{50} values (compound concentration that produces 50% of cell death) are ascertained. For correlation purposes, the cytotoxicity of fluorouracil (5-FU) and the metal complexes are assessed under the same test condition. It is clearly observed that the metal complex has a synergistic effect on the cytotoxicity (Table 3).

3.7.1. The cytotoxicity of complexes on epithelioid carcinoma cervix cancer (Hela) cell line

The assaying of cytotoxicity explains that the $[Co(tric\text{-}H)_2]\cdot0.5H_2O$ and $[Cd(tric)_2(Ac)_2]\cdot H_2O$ complexes have much lower IC_{50} value. While the complexes of $[Ni(tric)_2Cl_2(H_2O)_2]\cdot H_2O$, $[Ni(tric\text{-}H)_2(H_2O)_2]$, $[Co(tric)_2Cl_2]\cdot2.5H_2O$, and $[Cu(tric)_2]Cl_2\cdot3\,H_2O$ have a moderate IC_{50} value. The $[Zn(tric)_2Cl_2]\cdot EtOH$ complex has a weak IC_{50} value. The extent of the activities of these complexes lies between strong and moderate to weak.

3.7.2. The cytotoxicity of complexes on mammary gland breast cancer (MCF-7)

It is clearly observed that metal complex has a synergistic effect on the cytotoxicity (Table 3). The assaying of cytotoxicity explains that $[Co(tric\text{-}H)_2]\cdot0.5H_2O$ and $[Cd(tric)_2(Ac)_2]\cdot H_2O$ have much lower IC_{50} value. While $[Zn(tric)_2Cl_2]\cdot EtOH$, $[Ni(tric)_2Cl_2(H_2O)_2]\cdot H_2O$, $[Ni(tric\text{-}H)_2(H_2O)_2]$, $[Co(tric)_2Cl_2]\cdot2.5H_2O$, and $[Cu(tric)_2]Cl_2\cdot3\,H_2O$ have a higher IC_{50} value. The most extent of the activities of these complexes lies between strong to moderate as described in Figure 3.

Conflict of interest The authors declare that they have no conflict of interest.

References

[1] D. C. Crans, P. M. Ehde, P. K. Shin, and L. Pettersson, *Structural and kinetic characterization of simple complexes as models for vanadate-protein interactions*, J. Am. Chem. Soc., 113 (1991), 3728–3736.

[2] D. Chakraborty and P. K. Bhattacharya, *Intramolecular interligand interactions in Cu(II) ternary complexes involving dipeptides and amino acids*, J Inorg Biochem, 39 (1990), 1–8.

[3] V. Manjula, D. Chakraborty, and P. Bhattacharya, *Ternary complexes of Cu(II) involving histidine and another amino acid or dipeptide*, Indian J Chem, 29A (1990), 577–580.

[4] R. C. Kapoor, J. K. Jailwal, and J. Kishan, *Complex formation of N-[tris(hydroxymethyl)methyl]glycine with lead and cadmium*, J Inorg Nucl Chem, 40 (1978), 155–158.

[5] R. M. Tripathi, R. Ghose, and A. K. Ghose, *Heteroligand complexes of some transition metals containing 2,2'-bipyridyl and tricine as ligands in aqueous solution*, Indian J Chem, 24A (1985), 565–567.

[6] A. V. Vaidyan and P. K. Bhattacharya, *Interligand interaction in ternary complexes of Zn(II) and Cd(II) with dipeptides and aminoacids*, Can J Chem, 72 (1994), 1107–1110.
[7] B. de Castro, J. Pereira, P. Gameiro, and J. L. F. C. Lima, *Multinuclear NMR and potentiometric studies on the interaction of zinc and cadmium with cytidine and glycylglycine. The effect of the anion*, J Inorg Biochem, 45 (1992), 53–64.
[8] K. B. Pandeya and R. N. Patel, *Ternary complexes of copper(II) with glycylglycine, glycylglycylglycine and some imidazoles*, Indian J Chem, 29A (1990), 602–604.
[9] J. A. I. Kishan and R. Kapoor, *Complex formation of N-[tris(hydroxymethyl)methyl]glycine with copper(II) and zinc(II)*, Indian J Chem, 23A (1984), 355–356.
[10] E. Farkas and T. Kiss, *Effects of side-chain donor groups on deprotonation of peptide amide in copper(II) complexes at high pH*, Polyhedron, 8 (1989), 2463–2467.
[11] W. M. Hosny, *Complexes of vitamin B6. Ternary complexes of Cu(II) with pyridoxamine and amino acids, DNA units or peptides*, Egypt J Chem, 42 (1999), 151–173.
[12] E. Prenesti, P. G. Daniele, M. Prencipe, and G. Ostacoli, *Spectrum-structure correlation for visible absorption spectra of copper(II) complexes in aqueous solution*, Polyhedron, 18 (1999), 3233–3241.
[13] N. S. Al Radadi, S. M. A. Al Ashqar, and M. M. Mostafa, *Synthesis and characterization of some new binary and ternary Cu^{II} complexes*, Synth React Inorg Met-Org Nano-Met Chem, 41 (2011), 203–210.
[14] A. A. A. Boraei and I. T. Ahmed, *Divalent transition metal ion mixed-ligand complexes of tricine or glycylglycine and 8-hydroxyquinoline: synthesis, characterization, and formation constants*, Synth React Inorg Met-Org Nano-Met Chem, 32 (2002), 981–1000.
[15] O. M. El-Roudi, E. M. Abd Alla, and S. A. Ibrahim, *Potentiometric studies on the binary complexes of N-[tris(hydroxymethyl)methyl]glycine with Th^{4+}, Ce^{3+}, La^{3+}, and $UO_2{}^{2+}$ and medium effects on a Th-tricine binary complex*, J Chem Eng Data, 42 (1997), 609–613.
[16] K. Nakamoto, *Infrared and Raman Spectra of Inorganic and Coordination Compounds*, Wiley, New York, 5th ed., 1997.
[17] K. Ketcham, I. Garcia, J. Swearingen, A. El-Sawaf, E. Bermejo, A. Castineiras, et al., *Spectral studies and X-ray crystal structures of three nickel(II) complexes of 2-pyridineformamide 3-piperidylthiosemicarbazone*, Polyhedron, 21 (2002), 859–865.
[18] R. G. Bates, R. N. Roy, and R. A. Robinson, *Solute-solvent effects in the acidic dissociation of the ampholyte N-tris(hydroxymethyl)methylglycine ("tricine") in 50 mass % methanol-water solvent*, J Solution Chem, 3 (1974), 905–916.
[19] A. B. P. Lever, *Inorganic Electronic Spectroscopy*, Elsevier, Amsterdam, 1968.
[20] Y. Tanabe and S. Sugano, *On the absorption spectra of complex ions II*, J Phys Soc Jpn, 9 (1954), 766–779.
[21] A. Earnshaw, *Introduction to Magnetochemistry*, Academic Press, London, 1968.
[22] W. J. Geary, *The use of conductivity measurements in organic solvents for the characterisation of coordination compounds*, Coord Chem Rev, 7 (1971), 81–122.
[23] D. Kivelson and R. Neiman, *ESR studies on the bonding in copper complexes*, J Chem Phys, 35 (1961), 149–155.
[24] B. Singh, B. P. Yadava, and R. C. Aggarwal, *Synthesis and characterization of 1-phenyl-5-benzoyl-4-thiobiurate complexes with oxovanadium(IV), cobalt(II & III), nickel(II), copper(II), zinc(II), cadmium(II) and mercury(II)*, Indian J Chem, 23A (1984), 441–444.
[25] B. Delley, *An all-electron numerical method for solving the local density functional for polyatomic molecules*, J Chem Phys, 92 (1990), 508–517.
[26] B. Delley, *A scattering theoretic approach to scalar relativistic corrections on bonding*, Int J Quant Chem, 69 (1998), 423–433.
[27] B. Delley, *From molecules to solids with the $DMol^3$ approach*, J Chem Phys, 113 (2000), 7756–7764.
[28] X. Wu and A. K. Ray, *Density-functional study of water adsorption on the $PuO_{2(110)}$ surface*, Phys Rev B, 65 (2002), 085403.
[29] A. Kessi and B. Delley, *Density functional crystal vs. cluster models as applied to zeolites*, Int J Quant Chem, 68 (1998), 135–144.
[30] Accelrys Software Inc., *Materials Studio v5.0*, 2009.
[31] W. Linert and A. Taha, *Co-ordination of solvent molecules to square-planar mixed-ligand nickel(II) complexes: a thermodynamic and quantum-mechanical study*, J Chem Soc Dalton Trans, (1994), 1091–1095.
[32] I. Fridovich, *Superoxide anion radical (O_2^-), superoxide dismutases, and related matters*, J Biol Chem, 272 (1997), 18515–18517.
[33] I. Fridovich, *The biology of oxygen radicals*, Science, 201 (1978), 875–880.